

# The use of wavelet transform for an automated initialization in GPS/MEMS-IMU integration

*Hugues Fournier, Jan Skaloud, Adrian Waegli*  
Swiss Federal Institute of Technology, Lausanne

## BIOGRAPHY

*Hugues Fournier* obtained a M.Sc. in Geomatics Engineering from the Swiss Federal Institute of Technology, Lausanne for his work on the automated processing of the GPS/MEMS-IMU data. Currently he has joined the Swiss Federal Office of Topography where he works in the area of acquisition and maintenance of the Swiss topographic landscape model.

*Jan Skaloud* is senior scientist and lecturer at the Swiss Federal Institute of Technology, Lausanne. He holds a PhD. and M.Sc. in Geomatics Engineering from the University of Calgary and Dipl. Ing. in Surveying Engineering from the Czech Institute of Technology, Prague. He has been involved with GPS research and development since 1993 and has worked extensively on the integration of GPS and inertial navigation systems for precise airborne and terrestrial mapping.

*Adrian Waegli* holds a PhD. in computer, communication and information sciences and a M.Sc. in Geomatics Engineering from the Swiss Federal Institute of Technology, Lausanne. There, he got specialized for the integration of low-cost inertial and satellite navigation systems for trajectory determination.

## ABSTRACT

The main objective of this research is in automating the initialization phase of the MEMS-IMU/GPS data integration. The motivation for this study is the special case where the before mentioned sensors are worn on a body (e.g. of an athlete) and where the usually used static assumptions (i.e. zero velocity) are difficult to satisfy. Nevertheless, the proposed methodology is also applied on terrestrial vehicles with the aims of reducing the user interactions in the reconstruction of the trajectory from the recorded data. The proposed identification of dynamic versus (quasi) static periods is based on wavelet decomposition of the inertial measurements.

After presenting the bases of the process using the Continuous Wavelet Transform (CWT), the automated software's architecture is presented together with experiences carried in different dynamic environments. The trajectories calculated with the automated initialization are compared to those benefiting from the manual selection of the initialization periods based on experience and external knowledge of the underlying motion. As the differences between both approaches are negligible the new method is validated.

## INTRODUCTION

From a theoretical point of view, the employment of Global Navigation Satellite Systems (GNSS) such as GPS is sufficient for outdoors positioning. In reality, the reception of signals generated by satellites is sometimes disrupted or affected by obstructions, high dynamic, vibrations and multipath. This makes it difficult to maintain the high accuracy of GPS relative positioning for terrestrial applications that is otherwise experienced under good reception of satellite signals. In order to mitigate these effects, or even to bridge complete outages of GPS data, measurements of an Inertial Measurement Unit (IMU) are usually integrated with the satellite observations (Jekeli, 2001). Due to the ergonomic and cost constraints present in many applications (e.g. sports), a combination of sensors such as a single-frequency differential GPS and Micro Electro Mechanical System (MEMS)-IMUs have been used for continuous reconstruction of trajectories (Waegli and Skaloud, 2009).

Inertial navigation is an autonomous dead-reckoning method that has two distinct phases known as the initialization and the navigation phase. The initialization phase is difficult to achieve with the MEMS-IMU in general, and the situation is further complicated with the sensors worn on human beings. Indeed, the zero velocity assumption used for initialization and error estimation in inertial data for standing vehicles does not necessarily apply for body-worn sensors. Moreover, even if GPS data are available during the 'standing' phase, the small displacement

does not enable observing the systematic errors present in the MEMS-sensors, particularly the gyroscopes. Hence, it is better to separate the ‘quasi-static’ periods of longer duration from the rest of the data and remove them from the processing.

Such separation could be for instance made when the norm of the inertial measurements exceeds certain threshold. However, direct application of such approach is less feasible for MEMS-IMUs which noise level is generally high. Suppressing the noise-level prior the thresholding by a simple technique like moving average creates an additional problem as the precise identification of the transition phase is then difficult to localize (Waegli, 2009). Indeed, the quality of precise detection by this method is highly related to the compromise between the resolution and the noise reduction level. Tuning the computing parameters is fastidious, and thus this method is not flexible across various applications. Therefore, it appears necessary to find another way to properly isolate the ‘quasi-static’ phases for the purpose of initialization.

### Objectives

This study aims to improve the before mentioned approach by implementing an automated detection of the ‘quasi-static’ periods of a given signal into an existing navigation software (Waegli, 2009). The selected methodology should be valid across variety of applications and limit or completely avoid user interactions.

To reach this goal, a new strategy, based on the Continuous Wavelet Transform (CWT), was adopted. The new methodology analyses the CWT coefficients. This approach allows the calibration of the parameters for the detection of ‘quasi-static’ periods, based on the characteristics of the studied signal. Jointly, a new software architecture that minimizes the number of user interactions related to the initialization phase was implemented and evaluated.

### Outline

In the first three sections of this article, the problematic of automated initialization with body-worn MEMS-IMU/GPS sensors is exposed together with its requirements. Then, the theoretical bases of the CWT are introduced together with the analysis of its coefficients. Next, the implementation of the automated detection of the ‘quasi-static’ periods is presented in details. The fourth section briefly describes the various experiments and data sets used for testing. The validation of the new software is then presented using the before mentioned data sets. Finally, the paper concludes with a short discussion about the implemented method and proposes ideas for further developments.

## THE INITIALIZATION PHASE

With body-worn inertial sensors, the assumption of zero velocity is generalized to a case where the

position of a subject wearing the sensors does not change within a predefined threshold (e.g. dm or m level). Hence, each experimentation signal is composed of so called ‘quasi-static’ and ‘dynamic’ periods. Fig. 1 illustrates a signal where the ‘dynamic’ periods are emphasized with a grey background.

The first phase of the integration process is undertaken during the ‘quasi-static’ periods, and aims to compute the initial approximation of the sensor's position, velocity and attitude (PVA) states. Indeed, when the velocity is close to zero, the attitude can be computed by comparing the triad of MEMS-IMU's magnetic and accelerometer measurements in the body frame, with the local magnetic and normal gravity fields, respectively, expressed in local-level frame. The quaternion-based estimation algorithm QUEST (Psiaki, 1999) is implemented to compute the attitude by this approach, while the initial position and velocity are provided by the GPS receiver. The initialization phase is then followed by strapdown navigation and GPS/INS integration via Kalman filtering and smoothing leading to the optimal reconstruction of the trajectory.

In the existing implementation of the software (Waegli, 2009), the data ranges that are used to reconstitute the PVA evolution are manually selected by the user. To avoid such subjective and laborious interventions, it is necessary to develop a process which can automatically identify the time boundaries of the ‘dynamic’ periods and their associated ‘quasi-static’ ranges used for initialization.

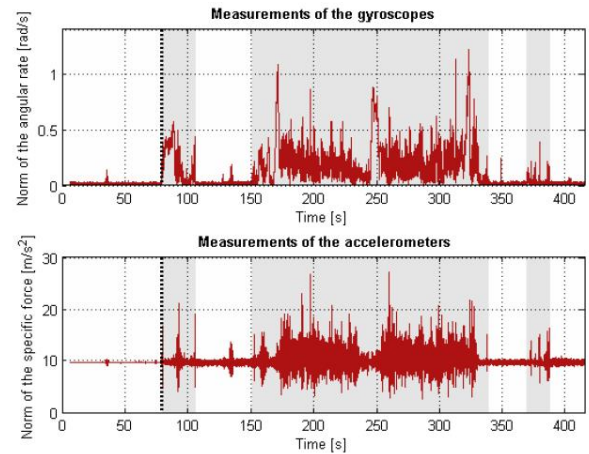


**Fig. 1 : Norm of gyroscopic and accelerometer signal on a motorbike.**

In order to perform a valid detection across various applications, it is necessary to choose a signal that is independent from IMU installation and vibration. In applications where the IMU is body-worn, the accelerometric signal seems to be better suited since high static rotations without translation may occur. On the other hand, the gyroscopic norm given by the

relation  $\|\omega_{ib}^b\| = \sqrt{(\omega_{ib,x}^b)^2 + (\omega_{ib,y}^b)^2 + (\omega_{ib,z}^b)^2}$  is applicable in wider sense as it is less perturbed by parasitic noise (i.e. motor vibrations) than the

accelerometer's measurements. This is illustrated on Fig. 1 where as soon as the motor is turned on (black vertical dotted line), the magnitude of the noise on the acceleration sensors increases, while it stays stable for the gyroscopic signal.

A specific treatment is reserved for each type of dynamic state. As previously mentioned, the biases of inertial sensors are difficult to observe during the 'quasi-static' periods with GPS data. Hence, the latter may evolve/drift significantly in time while its corresponding covariance in the Kalman Filter (KF) stays (more or less) stable due to the presence of updates. This may later lead to filter divergence when the velocity increases and orientation errors become again observable. Therefore, we prefer computing a new initialization during such periods rather than performing strapdown navigation. However, an adaptive process is necessary to distinguish the 'quasi-static' periods from the 'dynamic' ones whatever the type of the application (ski, motorbike, car, etc).

## THEORETICAL BACKGROUND FOR AUTOMATED INITIALIZATION

The use of moving average window could be an efficient method to automate the detection of the 'quasi-static' periods. However, this method does not provide enough flexibility, due to the compromise between the obtained resolution and the noise suppressing level when choosing the size of the window. Indeed, a large window size provides an important smoothing effect but does not enable sharp and accurate detection in the signal transition to/from higher dynamics. Thus, specific tuning of this parameter is required for each application, which makes the use of the moving average window less suitable for an automated initialization.

The CWT is frequently used to solve numerous scientific problems where the most important part of the information of a signal is contained in its irregularities (Mallat and Hwang, 1992). Indeed, this mathematical tool offers an analysis in time and frequency domains that enables an accurate localization of the signal's singularities. Schematically, this method consists of sliding a window stepwise along the analyzed signal and computing the signal's spectrum at each step. The complete time-frequency analysis is obtained by varying the size of the window (Valens, 1999).

The first step of the CWT consists in the choice of a mother wavelet, noted  $\psi(t)$ , that is used as basis function for representing other functions. The simplest mother function which satisfies the relation  $\int \psi(t) dt = 0$  is the Haar wavelet.

New wavelets can be generated by dilating and translating  $\psi(t)$ . The dilatation enables the analysis of the frequency scales, and the translation is used to analyze the time scale (Vidakovic and Mueller, 1994). The equation (1) describes the generation of new wavelets by this method:

$$\psi_{\tau,s}(t) = \frac{1}{s} \psi\left(\frac{t-\tau}{s}\right) \quad (1)$$

With:  $s$  = scale factor  
 $\tau$  = translation factor  
 $\psi$  = mother wavelet  
 $\psi_{\tau,s}(t)$  = generated wavelet

Through this approach it becomes possible to generate various wavelets, and describe the analyzed signal as a superposition of all of them (2):

$$f(t) = K \iint T(\tau,s) \psi_{\tau,s}(t) \delta\tau \frac{\delta s}{s} \quad (2)$$

With:  $K$  = constant dependant only of  $\psi(t)$   
 $T(\tau,s)$  = coefficients of the CWT

Equation (2) can also be inverted to obtain the coefficients of the CWT for a given function  $f(t)$ .

$$T(\tau,s) = \frac{1}{s} \iint f(t) \psi_{\tau,s}^*(t) \delta\tau \frac{\delta s}{s} \quad (3)$$

With:  $\psi^*$  = complex conjugate of  $\psi$

By applying equation (3) it is possible to obtain a CWT for every signal  $f(t)$ . The singularities contained in the signal will be expressed by high values of the corresponding coefficients in the CWT. Refining the analysis in the frequency scale gives an accurate time localization of the singularities, the reason for which the CTW is a very powerful in identifying transition periods even in the noisy signal. To illustrate this capability, a synthetic signal is generated and treated with the CWT. The coefficients obtained thereby are represented on a time-scale space in Fig. 2.

The lower part of Fig. 2 shows the theoretical signal composed of four distinct peaks, while the upper graph displays the corresponding coefficients. It clearly appears that the CWT is able to localize the singularities in a signal in time. Generally, short windows are able to detect only fast signal variations (i.e. high frequency), while large scales detect slow signal variations (i.e. low frequency) with a smoothing effect.

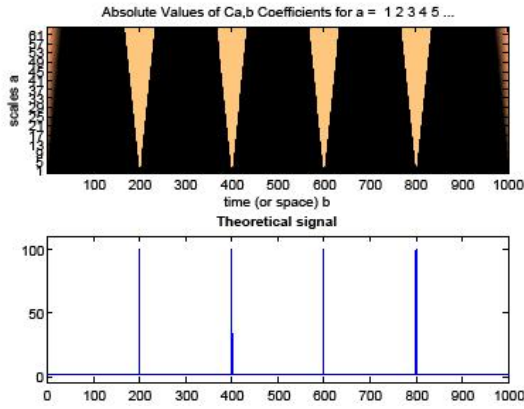


**Fig. 2 : CWT coefficients (top) of a synthetic signal (bottom).**

### ALGORITHM IMPLEMENTATION

The automated detection algorithm is composed of four main stages based on the CWT signal decomposition:

- First, the input data are de-noised using wavelets.
- Second, the CWT is applied to the de-noised signal, providing the CWT coefficients.
- Third, the CWT coefficients are smoothed with a spline and analyzed to detect the singularities of the studied signal. This is done using only the gyroscopic norm.
- Finally, the results of the first classification are confronted with the smoothed ground velocity acquired by GPS. This last step leads to the creation of a state vector containing the status of the dynamic at each time step of the experiment.

The mentioned processing steps are depicted in the work flow in Fig. 3 and will be explained later separately in more detail.

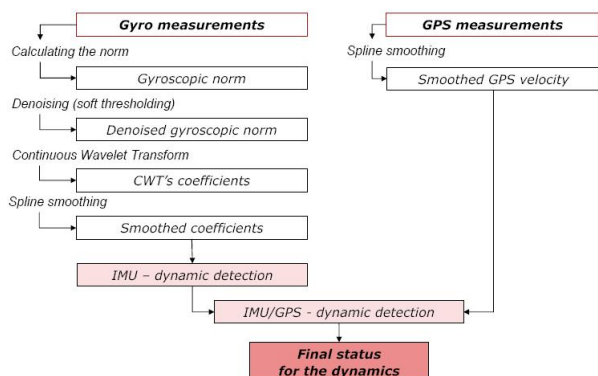


**Fig. 3 : Work flow for the automated detection of 'quasi-static' periods.**

### I. De-noising of the signal

The de-noising step is important in order to obtain a sharper detection with the CWT. De-noising by wavelet transform was chosen over classical spline smoothing because it preserves the characteristics of the underlying signal. Moreover, this approach has been shown to work well in a range of situations where many non-wavelets methods have met only partial success (Donoho, 1995).

The de-noising by wavelet transform, also called de-noising by soft-thresholding, is a procedure that aims to reject noise by thresholding the wavelet coefficients of the noisy signal. This treatment acts in three different stages:

- First, a wavelet transform analyzes the signal and yields the coefficients. The wavelet used for this type of application is a Daubechies 20 wavelet, because it is less discontinuous and may be better suited at representing smoother variations (Capilla, 2006).
- Then, the obtained coefficients are thresholded in order to reject the noise. An heuristic variant of the principle of Stein's Unbiased Risk Estimate (SURE) is used, because it is a near optimal method which uses an adaptive threshold selection. This thresholding process is well suited to recover a function of unknown smoothness from noisy sampled data (Donoho and Johnstone, 1995).
- Finally, an inverse wavelet transform rebuilds the de-noised signal, based on the thresholded coefficients.

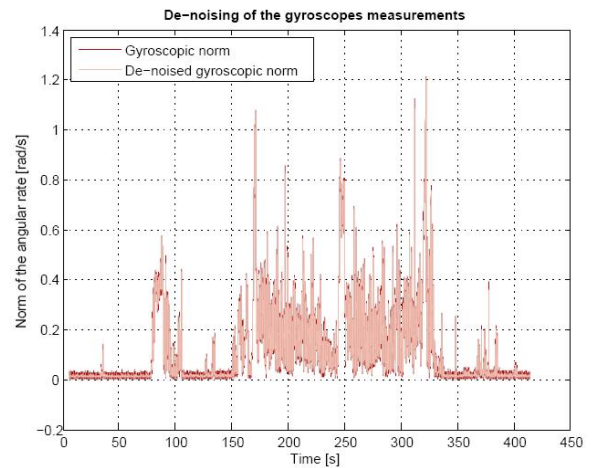


**Fig. 4 : De-noising of inertial data by soft thresholding.**

The entire process leads to an adaptive de-noising of the gyroscopic norm. Fig. 4 illustrates the result of de-noising inertial data by soft-thresholding. It can be seen in the figure that the characteristics of the signal are conserved. This would not be the case with a simple spline smoothing, which would distort the signal to a greater extent.

## II. Wavelet decomposition (CWT)

First, a mother wavelet must be chosen. For the detection of fast variations, the Haar wavelet appears to be well adapted, owing to its capacity to emphasize discontinuities in the raw data (Capilla, 2006).

The translations of the wavelet are limited by the duration of the signal, but the choice of dilatation is far more complex. To perform an optimal time-frequency analysis, a series of dilated wavelet is seen as a bank of band-pass filters on the signal (Valens, 1999).

To reduce as much as possible the computations, the adequate number of filters (dilatations) that are really needed is obtained with the following relation (4) (Capilla, 2006):

$$J = \log_2(N) \quad (4)$$

With:  $J$  = number of useful scales  
 $N$  = number of samples in the signal

Then, a selection is done among these useful scales to retain only the interesting frequencies for separating the ‘dynamic’ phases. Indeed, each time the signal passes through a filter its frequency is split in two. This is illustrated in Tab. 1 for measurements sampled at 100 Hz. Bold numbers show interesting frequencies that would be retained for application like alpine skiing (i.e. 0.1 to 10 Hz). Hence, CWT coefficients of the levels 4 to 10 will be used to localize the singularities.

Level	Frequency		Samples
	From [Hz]	To [Hz]	
1	50	100	N/2
2	25	50	N/4
3	12.5	25	N/8
4	<b>6.25</b>	<b>12.6</b>	<b>N/16</b>
5	<b>3.12</b>	<b>6.25</b>	<b>N/32</b>
6	<b>1.56</b>	<b>3.12</b>	<b>N/64</b>
7	<b>0.78</b>	<b>1.56</b>	<b>N/128</b>
8	<b>0.39</b>	<b>0.78</b>	<b>N/256</b>
9	<b>0.19</b>	<b>0.39</b>	<b>N/512</b>
10	<b>0.09</b>	<b>0.19</b>	<b>N/1024</b>
11	0.05	0.09	N/2048
12	0.02	0.05	N/4096
12	0	0.02	N/4096

**Tab. 1 : Application of a filter bank on a signal of length N sampled at 100Hz.**

In the cases of auto-moto applications such de-noising attenuates the perturbations caused by the motor's vibrations and thus provides a sharper detection. Note that the interesting frequency range for auto-moto applications is different from alpine skiing. Indeed, the higher inertia of a car implies lower acceleration and rotation rate than that of an athlete.

## III. Coefficient smoothing

To detect the singularities in the underlying signal an additional operation is required. The selected coefficients are squared and then summed to compute

the energy contained in the analyzed range of frequencies. This generates energy's coefficients vector that is smoothed with a spline. To detect the singularities, a soft thresholding is applied to this vector, taking the mean value of the smoothed coefficients as threshold. Values larger than the threshold are considered ‘dynamic’ and those below the threshold ‘quasi-static’.

## IV. Additional rules

Finally, the results of this detection based on IMU data are confronted with the GPS ground velocity measurements. According to detection rules presented in Tab. 2 the final classification of ‘dynamic’ phases is obtained.

Classification	Associated phase
IMU Quasi Static + GPS Dynamic	Navigation phase
IMU Quasi Static + GPS Quasi Static	Initialization phase
IMU Quasi Static + GPS Outage	Initialization phase
IMU Dynamic + GPS Dynamic	Navigation phase
IMU Dynamic + GPS Quasi Static	Initialization phase
IMU Dynamic + GPS Outage	Navigation phase
IMU Quasi Static only	Initialization phase
IMU Dynamic only	None

**Tab. 2 : Overview of the detection rules**

## RESULTS OF THE AUTOMATED PROCESS

Several practical tests were performed for the validation and evaluation of the automated approach. Various applications were considered in order to confront the proposed detection algorithm with several types of dynamics and assess its level of adaptability.

The low cost sensors were mounted together on the same support with a GPS antenna in order to know with precision the lever arm that separates their respective center. Two experiments were carried out with sensors directly mounted on vehicles (motorcycle and car). A third test was performed with the sensors mounted on the back of a skier, offering thus a totally different dynamics. Altogether, this will enable evaluating the capability of the automated detection algorithm within different applications.

### Validation of the new approach

To ensure that the automated algorithm works properly, its performances were evaluated by an approach that is schematically illustrated in Fig. 5. Each data set was processed twice, first using the manual version of the software and then with the automated separation of ‘dynamic’ periods. The obtained trajectories were compared and the validation was qualified as successful when the differences between both trajectories were negligible.



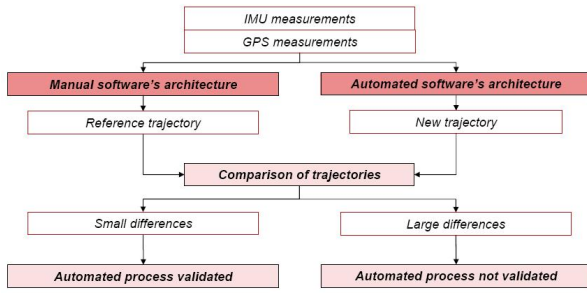


**Fig. 5 : Flow chart of the validation process.**

In all cases, the reference trajectory initiated on manually selected section of the data was practically identical to that calculated with the automated software. Indeed, as shown in Tab. 3 for one particular case, the differences in terms of position have a sub-centimeter mean value, with a standard deviation smaller than two centimeters.

		Mean	Median	SD	IQR
$\delta E$	[m]	0.001	0.001	0.014	0.003
$\delta N$	[m]	-0.003	-0.001	0.010	0.004
$\delta h$	[m]	0.005	0.005	0.006	0.002
$\delta LD$	[m]	0.008	0.005	0.018	0.005
$\delta v_h$	[m/s]	-0.001	-0.001	0.017	0.008
$\delta v_{3D}$	[m/s]	0.004	0.005	0.052	0.021

**Tab. 3 : Comparisons of trajectories computed with the manual and the automated software's architecture ( $\delta E$ ,  $\delta N$ ,  $\delta h$  are the differences in East, Nord and height, respectively,  $\delta LD$  is the lateral displacement,  $\delta v_h$ ,  $\delta v_{3D}$  are differences in vertical velocity and 3D velocities).**

As the overall results calculated with the automated version of the GPS/INS software are very close to those obtained using the 'manual' version, it can be concluded that the automated algorithm works correctly. Therefore, the implemented approach is validated.

#### Example of detection

This section presents the results of several automated detections performed for ski, motorbike and car applications. Each experiment is depicted in Fig. 6 with three graphs, one per sampled signal. 'Dynamic' ranges are plotted in green and 'quasi-static' periods in red.

A visual inspection of plot in Fig. 6 confirms that the 'dynamic' ranges are well identified by the detection algorithm across different applications. This is especially true for the third example, where the sensors are fixed on a car which is far more stable during the static periods than a motorbike or athlete. As this experiment is more contrasted the automated detection of the static periods is completed reliable.

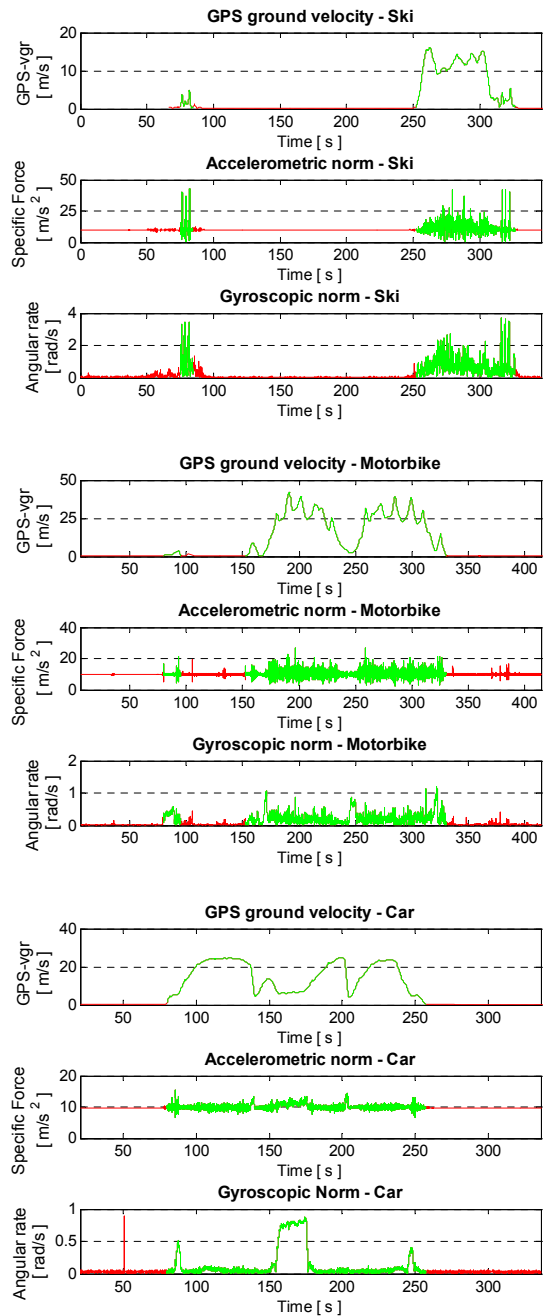


**Fig. 6 : Results of the automated detection for ski (top), motorbike (middle) and car (bottom) applications.**

## DISCUSSION

In the studied examples the proposed detection of static periods was sharp and accurate. That means that is applicable across different applications without additional tuning of parameters. Hence, the interaction of a user for this purpose is not longer necessary and the processing can be automated.

The analysis of coefficients across frequency ranges makes the proposed approach applicable to signals in a vibrating environment. The CWT technique is therefore appropriate also for the applications using motorized vehicles, in contrary to the moving average method.

Finally, future research should be oriented towards the qualitative evaluation of the static periods used for the initialization. Each period could have a quality index associated, which is later used in adapting the initial covariance of the estimated orientation prior the navigation phase.

## CONCLUSION

The presented approach provides an interesting alternative for an automated detection of the 'quasi-static' periods in low-cost GPS/MEMS-IMU integration. This reduces the number of interactions made by the user in the reconstruction of trajectories from the recorded data. The proposed method is based on the analyses of the CWT coefficients and appears to work correctly across various sport applications without tedious tuning of the computational parameters.

Trajectories calculated based on the automated detection were close to those obtained by the 'best' manual selection. This validates the new approach as well as its implementation, and encourages further developments towards a black-box system based on GPS/MEMS-IMU sensors in sports.

## ACKNOWLEDGEMENTS

The authors greatly appreciate the support of Christian Baumann, Florence Bonvin and Yannick Stebler for their courageous performances during the acquisition of the new datasets.

## REFERENCES

Capilla, C. (2006). Application of the Haar wavelet transform to detect microseismic signal arrivals. *Journal of Applied Geophysics*, Vol. 59, pages 36-46.

Donoho, D.L. (1995). De-noising by soft-thresholding. *IEEE Transactions on Information Theory*, Vol. 41, pages 613-627.

Donoho, D.L. and Johnstone, I.M. (1995). Adapting to unknown smoothness via wavelet shrinkage. *Journal of the American Statistical Association*, Vol. 90, pages 1200-1224.

Jekeli, C. (2001). Inertial navigation systems with geodetic applications. *Walter de Gruyter*, Berlin.

Mallat, S. and Hwang, W.L. (1992). Singularity detection and processing with wavelets. *IEEE Transactions on Information Theory*, Vol. 38, pages 617-643.

Psiaki, M.L. (1999). Extended quest attitude determination filtering, Cornell University, 1999.

Valens, C. (1999). A Really Friendly Guide to Wavelets.

Vidakovic, B. and Mueller, P. (1994). Wavelets for kids, A Tutorial Introduction. *Discussion paper*. Duke University 1994.

Waegli, A. (2009). Trajectory Determination and Analysis in Sports by Satellite and Inertial Navigation. *PhD thesis No. 4288*, EPFL 2009.

Waegli, A. and Skaloud J. (2009). Optimization of two GPS/MEMS-IMU integration strategies with application to sports, *GPS Solutions*, DOI 10.1007/s10291-009-0124-5.